Supplementary Figures

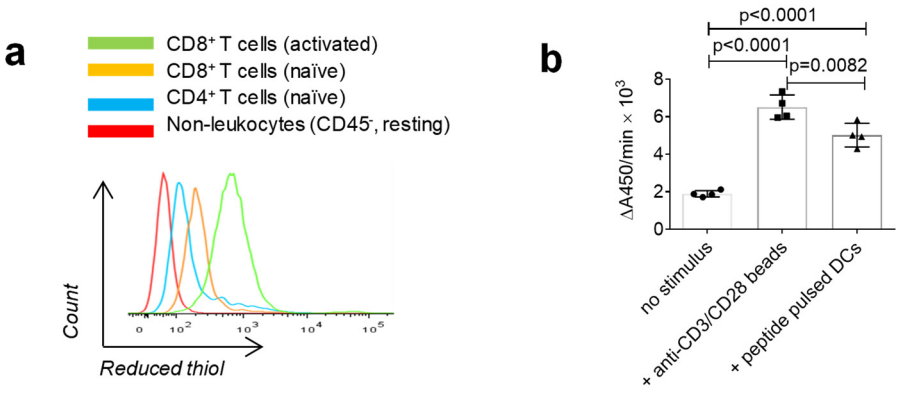

Supplementary Fig. 1. Surface thiol groups and reduction of activated T cells. (**a**) Activated $CD8^+$ T-cells have high expression levels of free thiol groups on cell surface proteins. $CD4^+$ or $CD8^+$ T-cells isolated from spleens of C57Bl/6 mice were either directly stained with an Alexa fluor 488-maleimide conjugate or $CD8^+$ T-cells were primed with con-A and IL-7 and then stained with Alexa fluor 488-maleimide and analyzed by flow cytometry. (**b**) Con-A-primed $CD8^+$ T cells were incubated with or without peptide pulsed DC or anti-CD3/CD28 beads for 24 hrs followed by similar WST-1 assay for the measurement of cell surface reduction activity. Data represent the mean ± s.e.m. (n = 3) and analysed by One-Way ANOVA and Tukey's tests. Shown are one representative of at least two independent experiments.

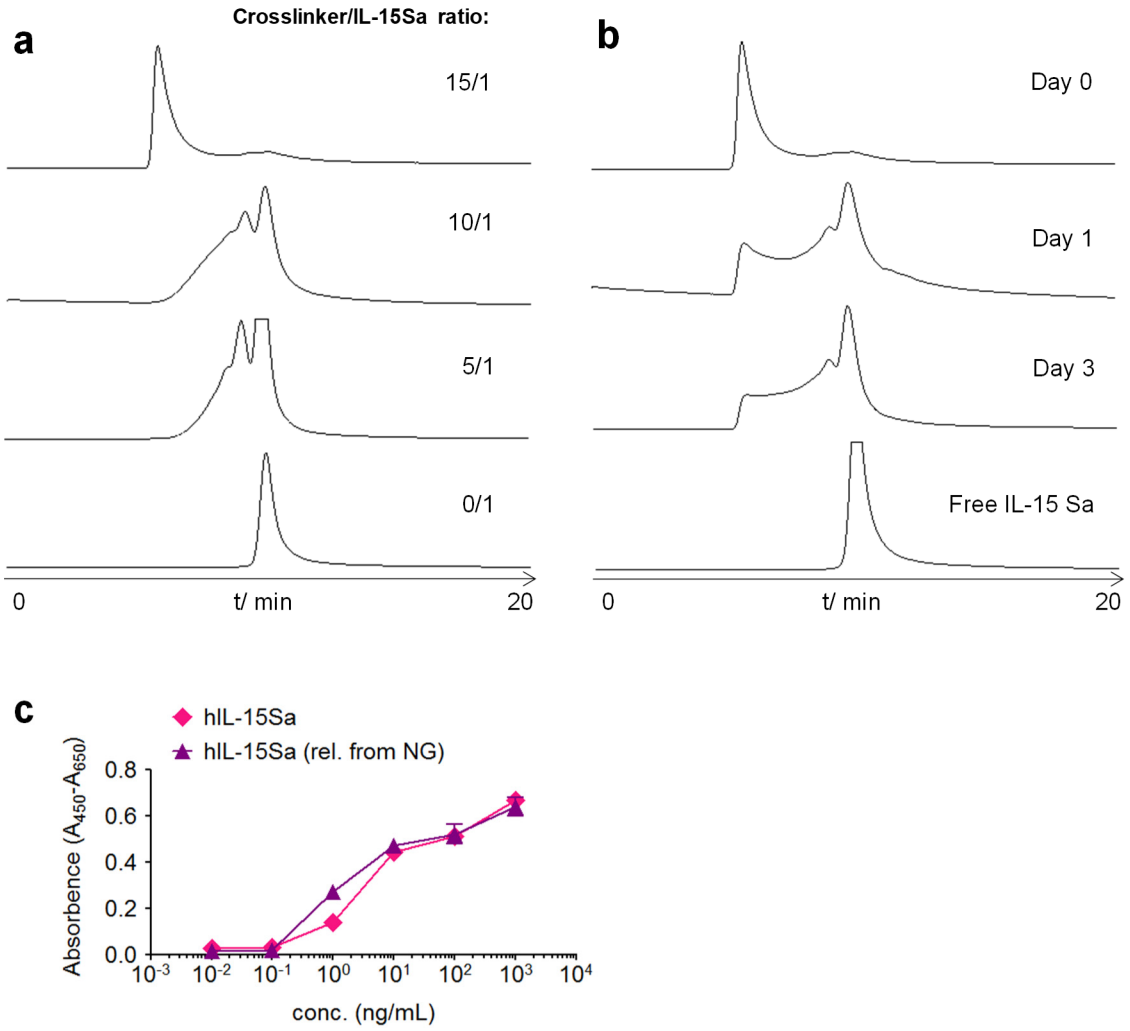

Supplementary Fig. 2. Characteristics of protein nanogel formation and disassembly. (**a**) HPLC characterization of nanogels formed with different NHS-SS-NHS to IL-15Sa ratios as indicated. (**b**) HPLC characterization of released IL-15Sa from at different days (labeled on the chromatography traces) in solution with GSH (1 mM). (**c**) Comparison of the bioactivity of fresh IL-15Sa vs. cytokine released from nanogels via CTLL-2 proliferation assay. Shown are one representative of at least two independent experiments.

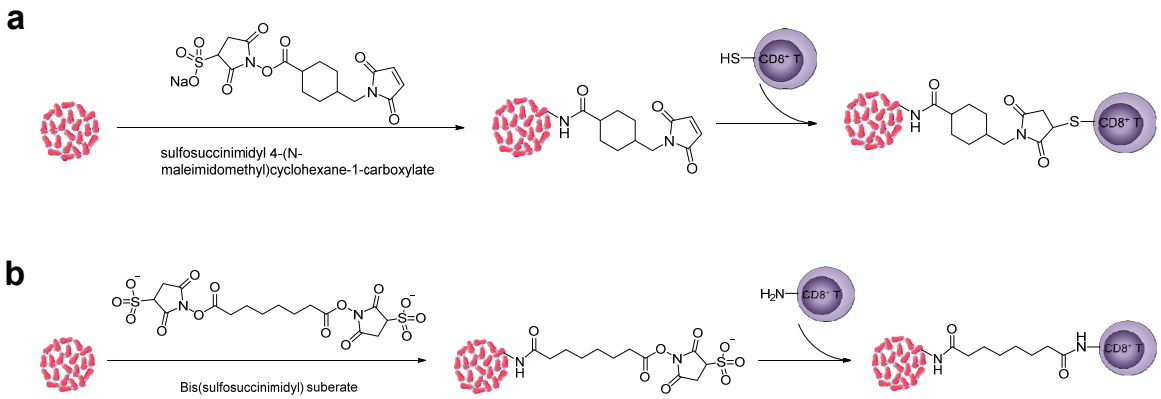

Supplementary Fig. 3. Conjugation of cytokine NGs to CD8$^+$ T-cells through covalent linkers. (**a**) NG is modified with sulfosuccinimidyl 4-(N-maleimidomethyl) cyclohexane-1-carboxylate and then conjugated to the free thiol groups on CD8$^+$ T-cell surfaces. (**b**) NG is modified with bis(sulfosuccinimidyl) suberate and then conjugated to the amine groups on CD8$^+$ T-cell surfaces.

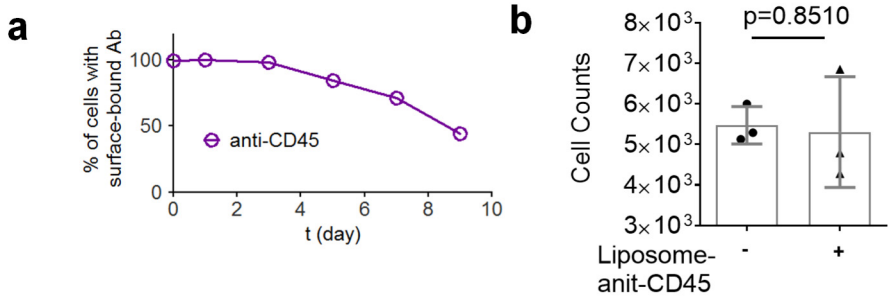

Supplementary Fig. 4. CD45 is slowly internalized and CD45 crosslinking by nanoparticles does not alter T-cell proliferative responses to TCR triggering. (**a**) Primed pmel-1 CD8$^+$ T-cells were stained with 171 μg/mL biotinylated anti-CD45 and levels of cell surface-localized antibody over time were detected by streptavidin staining and flow cytometry analysis. (**b**) Activated mouse CD8$^+$ T-cells stimulated with anti-CD3/CD28 beads and IL-2 were incubated with or without anti-CD45-liposomes (0.2 μg/mL equivalent antibody concentration). After 2 days, cells were counted by flow cytometry with counting beads. Data represent the mean ± s.e.m. (n = 3) and analysed by One-Way ANOVA and Tukey's tests. Shown are one representative of at least two independent experiments.

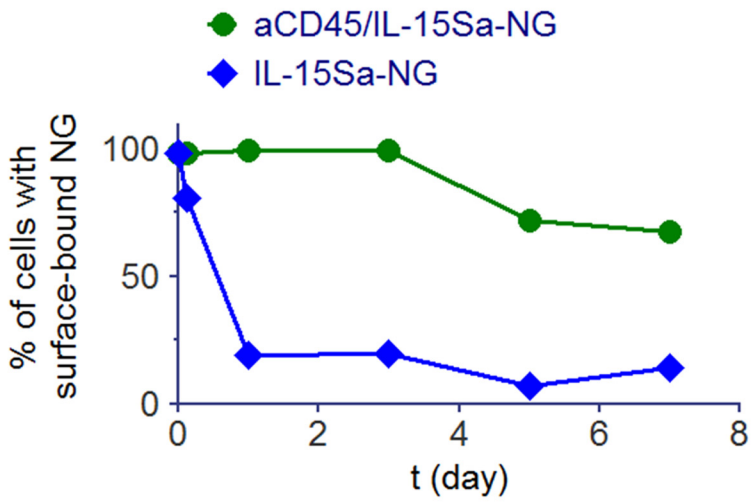

Supplementary Fig. 5. Anti-CD45 provides stable cell surface coupling of human CD8$^+$ T cells with NG backpacks. Primed human CD8$^+$ T-cells were conjugated with anti-human CD45/IL-15Sa biotinylated nanogels or IL-15Sa biotinylated nanogels, and the proportion of cells retaining surface-accessible NGs was followed over time by staining with fluorescent streptavidin followed by flow cytometry analysis. Shown are one representative of two independent experiments.

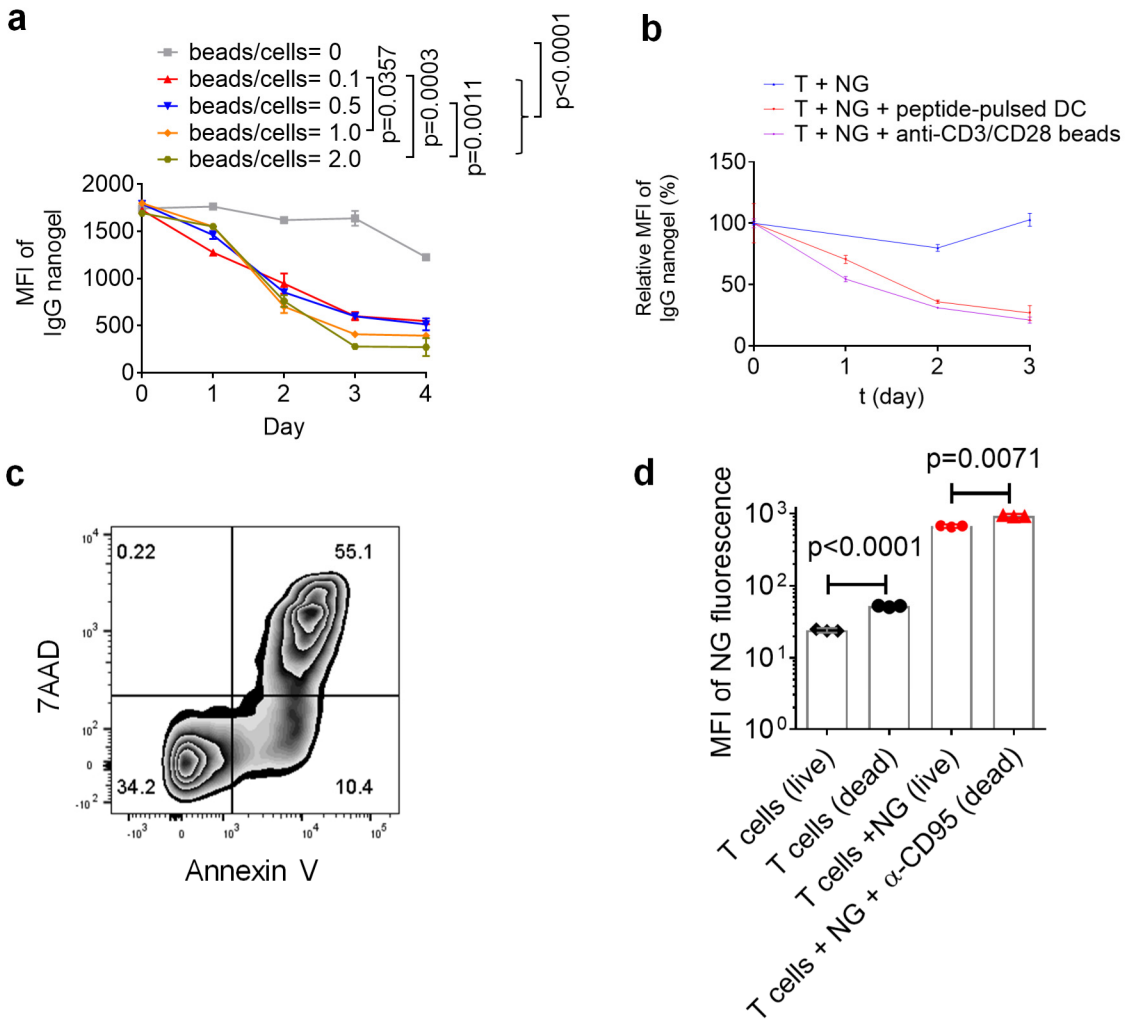

Supplementary Fig. 6. Nanogels dissolve in response to TCR stimulation by anti-CD3 or antigen presenting cells but not during apoptosis. (**a**) Alexa Fluor 647-labeled aCD45/IgG-NG (10 µg/10^6 T-cells) were prepared and coupled to primed polyclonal C57Bl/6 $CD8^+$ T-cells. T-cells were incubated in media at 37°C with anti-CD3/CD28 beads at various bead:T-cell ratios. Cell were collected at selected time points and analysed with flow cytometry for measurement of mean fluorescence intensity (MFI) over time. Data represent the mean ± SD (n = 3). (**b**) Release kinetics of human IgG from IgG nanogel-backpacked pmel T cells incubated with or without gp100 peptide-pulsed DCs as assessed by flow cytometry measurement of cell-associated geometric mean nanogel fluorescence. Data represent the mean ± SD (n = 3). (**c, d**) Primed C57Bl/6 $CD8^+$ T-cells alone or with surface-conjugated aCD45/IL-15Sa -NGs were incubated in complete RPMI at 37°C for 3 hrs with or without 10 µg/mL anti-CD95, then washed and cultured an additional hour followed by flow cytometry analysis. (**c**) Representative flow cytometry plot showing apoptotic $CD8^+$ T-cells with NG backpacks after incubation with

anti-CD95. (**d**) Geometric mean fluorescence intensity of NG channel shown for live T-cells, dead T-cells, live T-cells with NG backpacks and dead T-cells with NG backpacks after incubation with anti-CD95. Data represent the mean ± 95% confidence interval (n = 3). All data are analysed by One-Way ANOVA and Tukey's tests. Shown are one representative of at least two independent experiments.

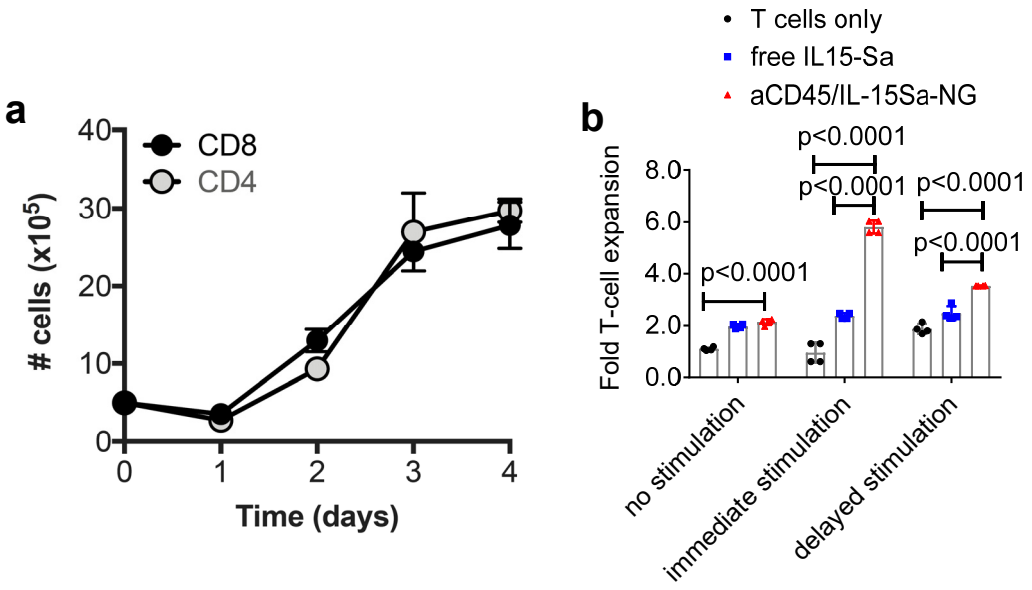

Supplementary Fig. 7. In vitro T cell expansion by nanogel IL-15Sa. (**a**) IL -15Sa nanogels expanded both $CD4^+$ and $CD8^+$ T cells. Naïve polyclonal C57Bl/6 $CD8^+$ and $CD4^+$ T cells were isolated from splenocytes and primed with anti-CD3/CD-28, then backpacked with aCD45/IL-15Sa-NGs (3.6 µg IL-15Sa/10^6 cells) and replated with anti-CD3/CD28 beads *in vitro*. Cell expansion over 4 days was followed by viable cell counting. (**b**) Polyclonal C57Bl/6 $CD8^+$ T-cells were placed in culture in the presence of anti-CD3/CD28 beads for 3 days ("immediate stimulation") or were culture for 3 days with IL-7 (20 ng/mL) prior to addition of anti-CD3/CD28 beads for 3 days ("delayed stimulation"), or as a control were left unstimulated for 3 days, and the fold expansion of the cells in each condition compared to the unstimulated control cells was calculated. Three groups were compared: naïve $CD8^+$ T-cells alone, T-cells + free IL-15Sa (7.5 µg IL-15Sa/10^6 cells), or T-cells backpacked with aCD45/IL-15Sa-NGs at equivalent dose. Shown are means ± s.e.m. (n = 3 /group). Data are analysed by One-Way ANOVA and Tukey's tests. Shown are one representative of at least two independent experiments.

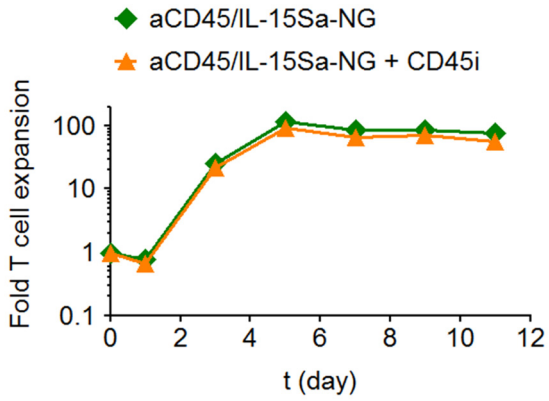

Supplementary Fig. 8. T-cell expansion induced by aCD45/IL-15Sa nanogels is not impacted by inhibition of CD45 phosphatase activity. Naïve C57Bl/6 $CD8^+$ T-cells were stimulated with anti-CD3/CD28 beads in the presence of surface bound aCD45/IL-15Sa-NGs, with or without 150 nM CD45 inhibitor (CD45i) added to the culture, and relative T-cell numbers were quantified over time. Shown are one representative of two independent experiments.

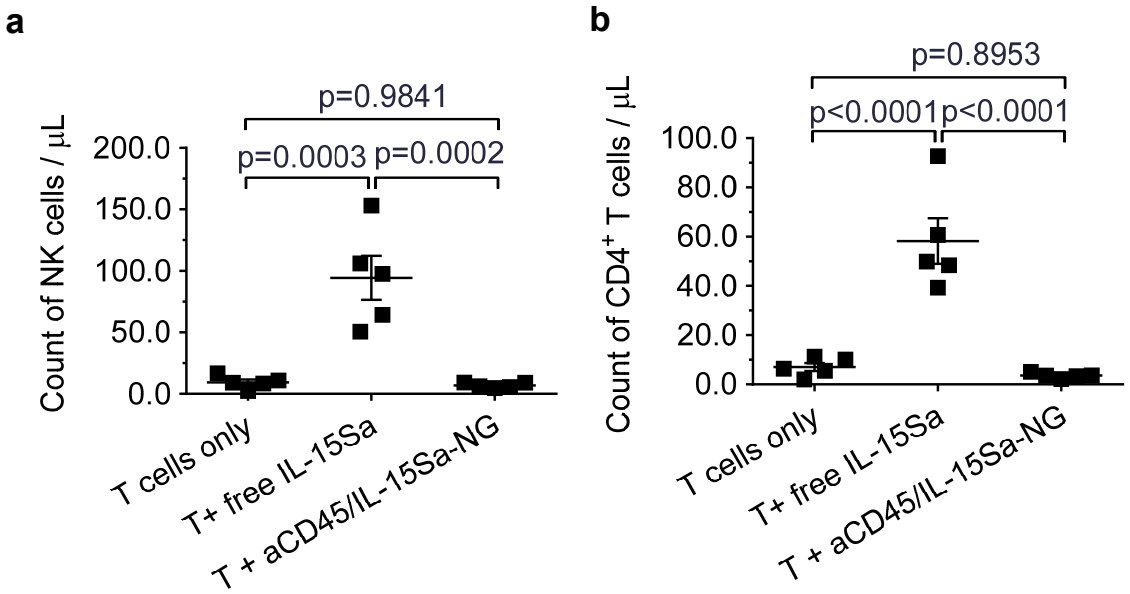

Supplementary Fig. 9. Free IL-15Sa but not IL-15Sa in nanogels backpack form expands NK cells and $CD4^+$ T-cells in the blood. Groups of B16F10 tumour-bearing mice received adoptive transfer of pmel-1 $CD8^+$ T-cells as described in **Figure 4**, and lymphocyte counts in peripheral blood were determined on day 14. Shown are counts of NK cells (**a**) and $CD4^+$ T-cells (**b**) in blood (normalized by volume) in different groups.

Shown are means ± s.e.m. (n = 5 /group). Data are analysed by One-Way ANOVA and Tukey's tests. Shown are one representative of two independent experiments.

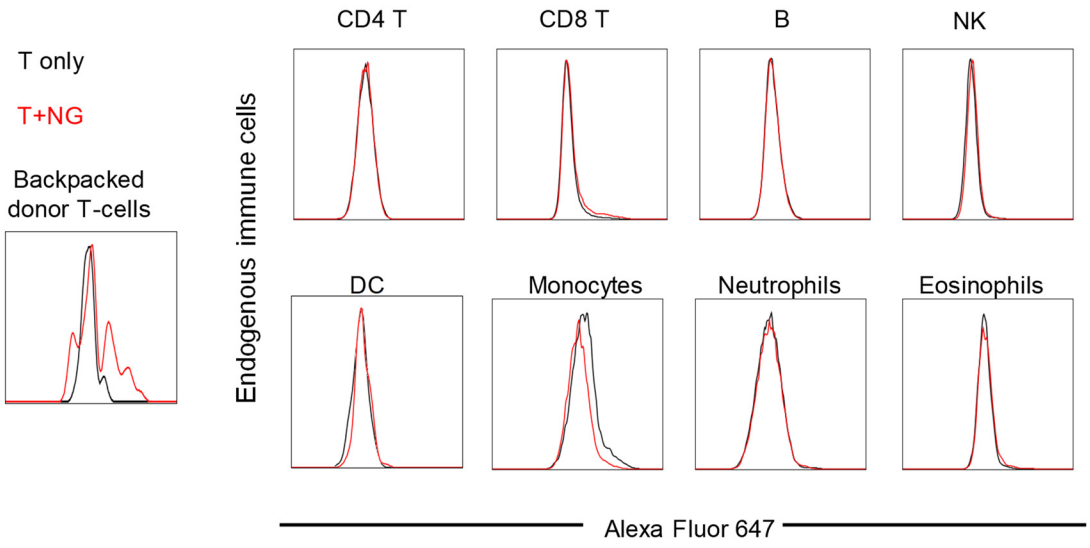

Supplementary Fig. 10. Nanogels show minimal transfer to endogenous immune cells *in vivo*. C57Bl/6 mice (*n* = 3/group) were injected with 5×10^6 primed pmel-1 Thy1.1$^+$CD8$^+$ T-cells with or without cell surface-conjugated Alexa Fluor 647-labeled aCD45/IL-15Sa-Gs (5 µg/10^6 T-cells) on day 0. On day 2, peripheral blood was collected and analysed by flow cytometry. Shown are representative flow cytometry histograms of NG fluorescence associated with transferred T cells, endogenous T cells, B cells, NK cells, and innate immune cells. Shown are one representative of two independent experiments.

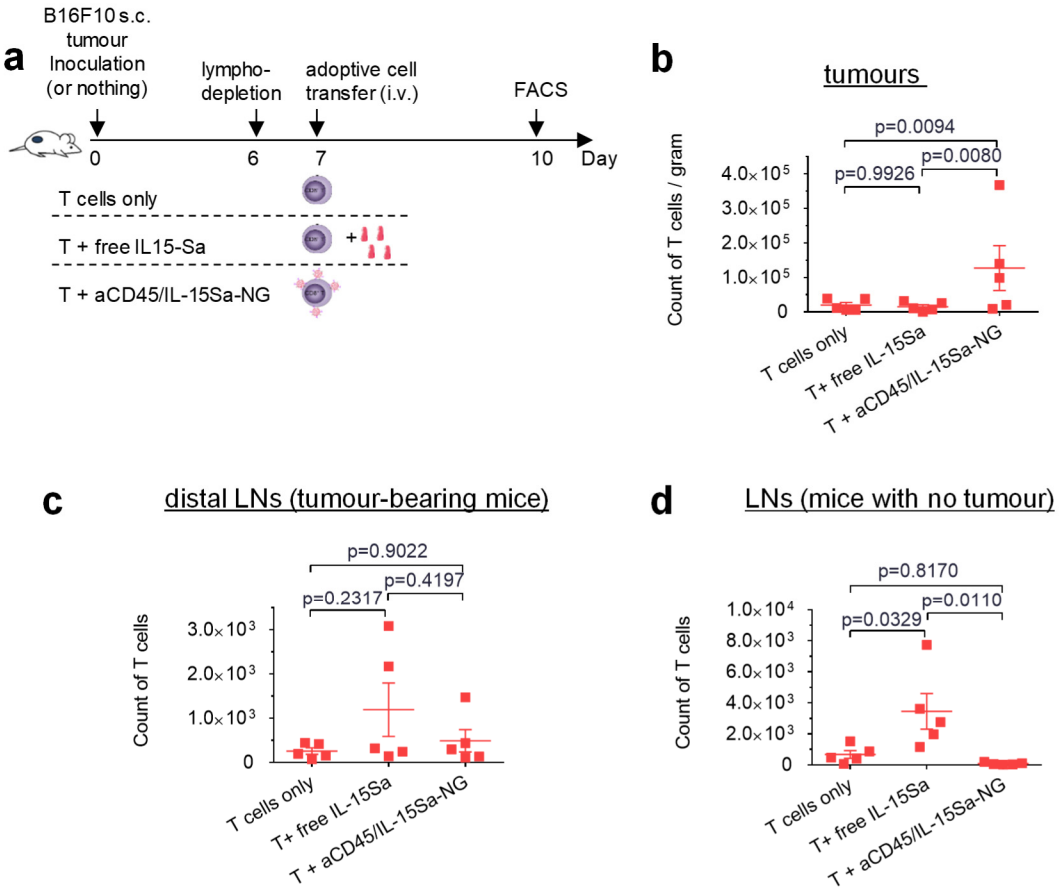

Supplementary Fig. 11. IL-15Sa-NGs promote expansion of adoptively transferred T-cells in tumours but not in distal lymphoid organs or tumour-free animals. B16F10 tumour cells (0.5×10^6) were injected s.c. in Thy1.2$^+$ C57Bl/6 mice and allowed to establish for 6 days. Animals were then sublethally lymphodepleted by irradiation on day 6 and received i.v. adoptive transfer of 10×10^6 primed pmel-1 Thy1.1$^+$CD8$^+$ T-cells on day 7. Treatment groups included T-cells alone, T-cells followed by a systemic injection of free IL-15Sa (40 µg), and T-cells coupled with aCD45/IL-15Sa-NGs (40 µg). On day 10, mice were sacrificed and tissues were processed and analysed by flow cytometry. (**a**) Timeline of study. (**b-c**) Counts of adoptively transferred (ACT) Thy1.1$^+$CD8$^+$ T-cells in tumours (**b**) and distal non-tumour draining lymph nodes (**c**, distal LNs). (**d**) C57Bl/6 mice without tumours received the same treatment; shown are counts of ACT Thy1.1$^+$CD8$^+$ T-cells in lymph nodes. Shown are one representative of two independent experiments. Data represent the mean ± s.e.m. (n = 5/group) and are analysed by One-Way ANOVA and Tukey's tests. Shown are one representative of two independent experiments.

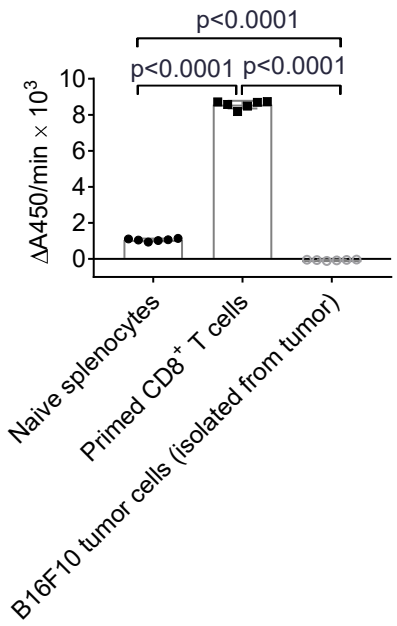

Supplementary Fig. 12. B16F10 tumour cells are not reductive. B16F10 cells (1×10^5) were implanted s.c. and allowed to establish tumours in C57Bl/6 mice for 20 days. Tumours were then excised, digested, and isolated B16 cells were placed in culture and the reduction rate of WST-1 in the presence of an intermediate electron acceptor was measured for 1 hr at 37°C. Data represent the mean ± SD. (n = 6/group) and are analysed by One-Way ANOVA and Tukey's tests. Shown are one representative of two independent experiments.

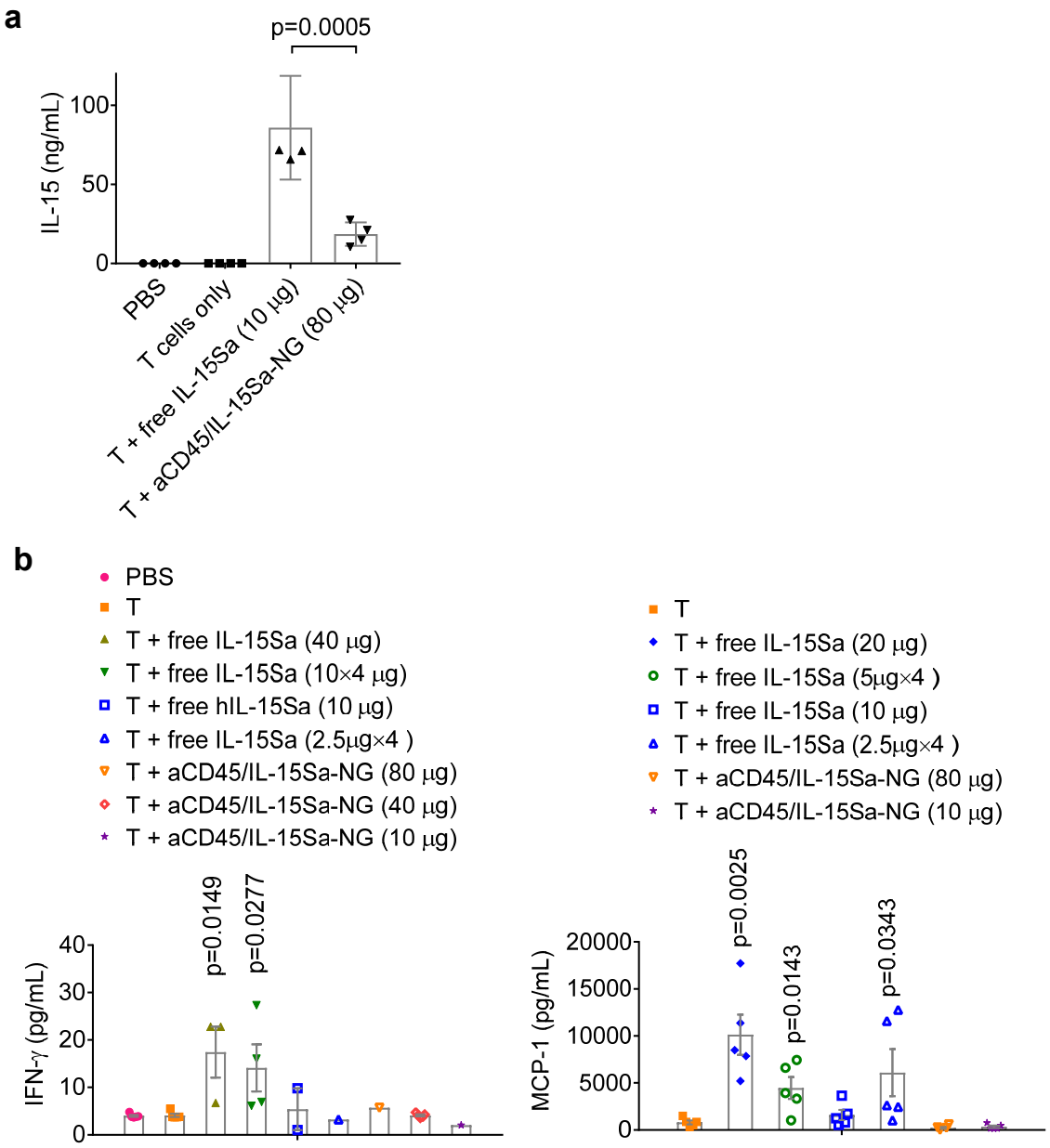

Supplementary Fig. 13. Free IL-15Sa but not IL-15Sa backpacks showed high serum levels of IL-15Sa in treated micee and elicits systemic inflammatory cytokines and chemokines. (**a**) B16F10 tumour cells (0.1×10^6) were injected s.c. in Thy1.2$^+$ C57Bl/6 mice and allowed to establish for 6 days. Animals were then sublethally lymphodepleted by irradiation on day 6 and received i.v. adoptive transfer of 10×10^6 gp100 peptide-activated pmel-1 Thy1.1$^+$CD8$^+$ T-cells on days 7 and 14. Animals received sham injections of PBS, T-cells only, T-cells with 10 µg i.v. injected free IL-15Sa, or T-cells with backpacked aCD45/IL-15Sa-NG (80 µg). Blood was draw on Day 16 and serum level of IL-15Sa was measure with human IL15/IL15RA ELISA kit. Data represent the mean ± s.e.m. (n = 4/group). (**b**) B16F10 tumour cells (0.5×10^6) were

injected s.c. into Thy1.2^{+} C57Bl/6 mice on day 0 and allowed to establish tumours for 6 days. Animals were then sublethally lymphodepleted by irradiation on day 6 and received i.v. adoptive transfer of 10 × 10^{6} activated pmel-1 Thy1.1^{+}CD8^{+} T-cells on day 7. For NG groups, T-cells were coupled with aCD45/IL-15Sa-NG at different doses right before adoptive transfer. Other groups of mice receive PBS, T-cells only or T-cells with different doses of i.v. injected free IL-15Sa as single dose (immediately after adoptive transfer) or multiple doses (Day 7, 10, 13 and 16). Serum cytokine levels were measured on day 17 or when the mice were sacrificed due to toxicity. Data represent the mean ± s.e.m. (n = 5) and are compared with control group (T cells only) for statistical analysis using One-Way ANOVA and Tukey's tests.

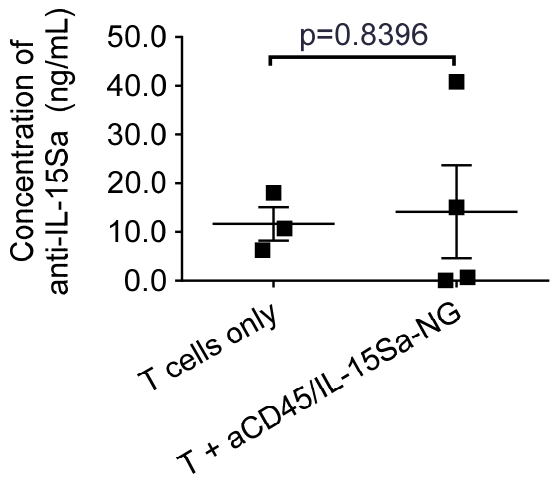

Supplementary Fig. 14. No anti-IL-15Sa humoral response is detected following NG backpack therapy in tumour-bearing mice. Serum from groups of C57Bl/6 mice treated as in **Figure 6** was collected and analyzed by ELISA for the presence of anti-IL-15Sa antibodies, with calibration from a monoclonal anti-human IL-15. Serum was collected from treated mice in different groups at 30 days post injection. Data represent the mean ± s.e.m. (n = 3) and are analysed by One-Way ANOVA and Tukey's tests.

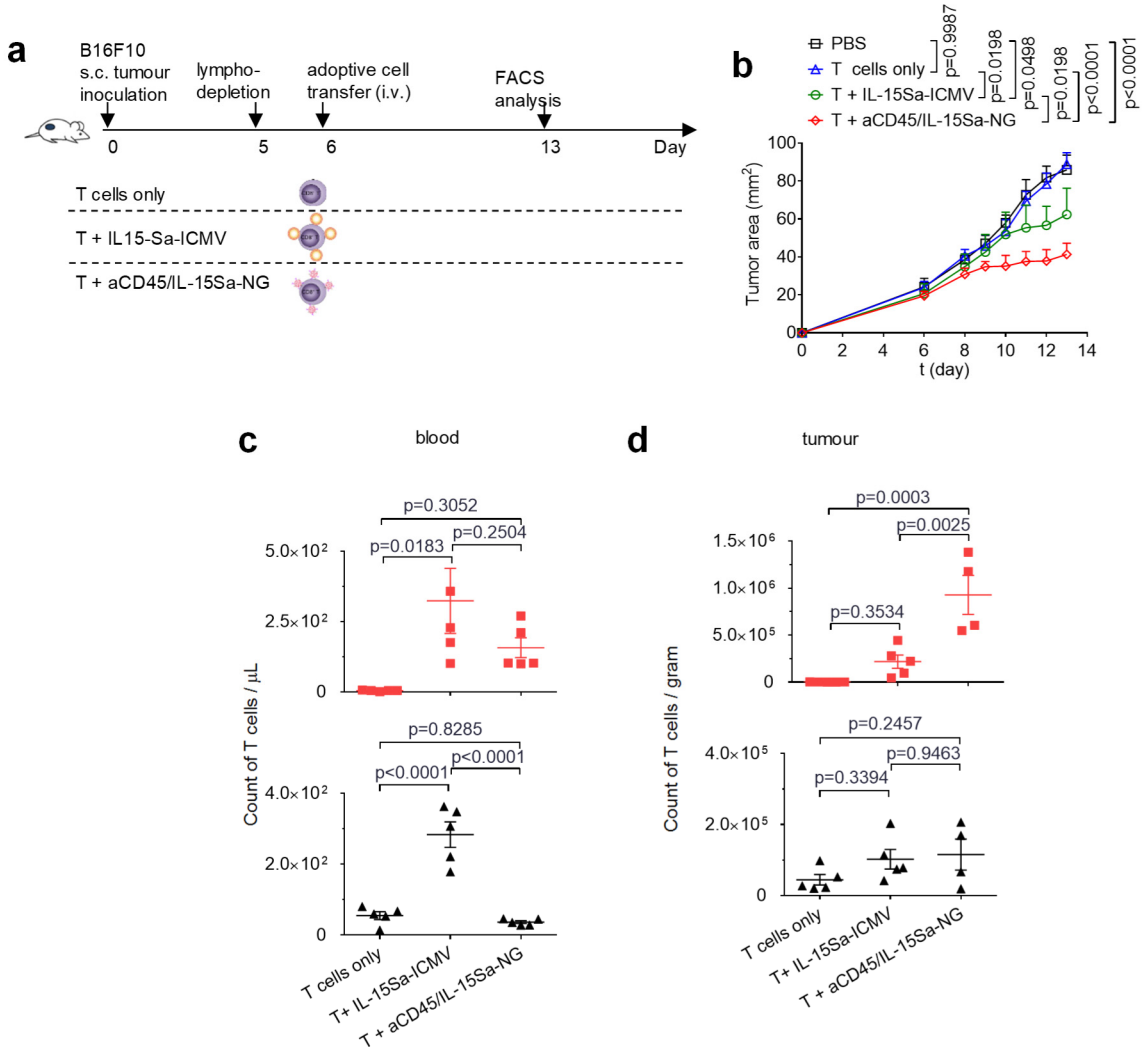

Supplementary Fig. 15 Nanogel backpacks outperform ICMV lipid capsules for IL-15Sa delivery to ACT T-cells *in vivo*. B16F10 tumour cells (0.5×10^6) were injected s.c. in Thy1.2$^+$ C57Bl/6 mice (n = 5/group) and allowed to establish for 5 days. Animals were then sublethally lymphodepleted by irradiation on day 5 and received i.v. adoptive transfer of 13.5×10^6 activated pmel-1 Thy1.1$^+$CD8$^+$ T-cells on day 6. Animals received sham injections of PBS, T-cells only, IL-15Sa-ICMV-backpacked T-cells (56 µg IL-15Sa), or aCD45/IL-15Sa-NG-backpacked T-cells (56 µg IL-15Sa). On day 13, mice were sacrificed and tissues were processed and analysed by flow cytometry. Shown are average tumour growth curves of each treatment group (**b**), and cell counts of transferred ACT T-cells (red squares) or endogenous CD8+ T-cells (black triangles) in blood (**c**) and tumours (**d**). Data represent the mean ± s.e.m. and are One-Way ANOVA and Tukey's tests.

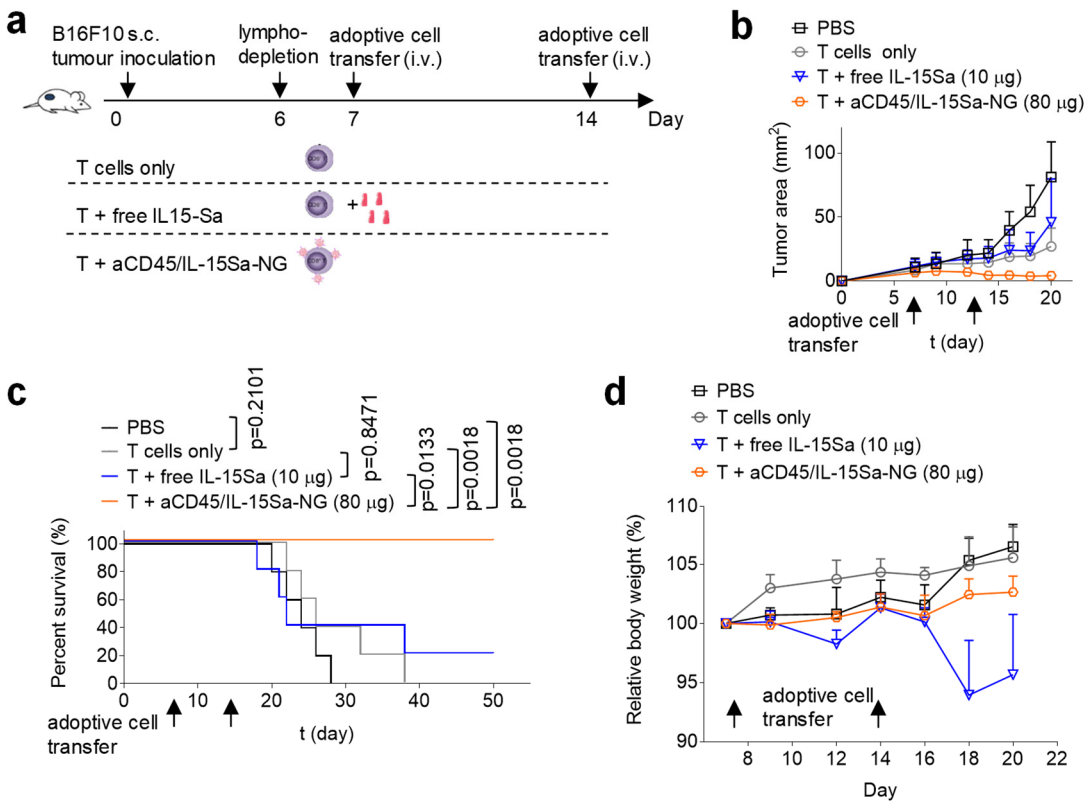

Supplementary Fig. 16. T Enhanced tumour elimination by repeat infusions of nanogel-loaded T-cells. (**a**) B16F10 tumour cells (0.1×10^6) were injected s.c. in Thy1.2$^+$ C57Bl/6 mice (n = 5/group) and allowed to establish for 6 days. Animals were then sublethally lymphodepleted by irradiation on day 6 and received i.v. adoptive transfer of 10×10^6 gp100 peptide-activated pmel-1 Thy1.1$^+$CD8$^+$ T-cells on days 7 and 14. Animals received sham injections of PBS, T-cells only, T-cells with 10 μg i.v. injected free IL-15Sa, or T-cells with backpacked aCD45/IL-15Sa-NG (80 μg). Shown are average tumour growth curves (**b**), survival curves (**c**), and percentage of body weight over time. Statistical analyses were performed using Two-Way ANOVA test for tumour growth data and Log-rank test for survival curves. Data represent the mean ± s.e.m..

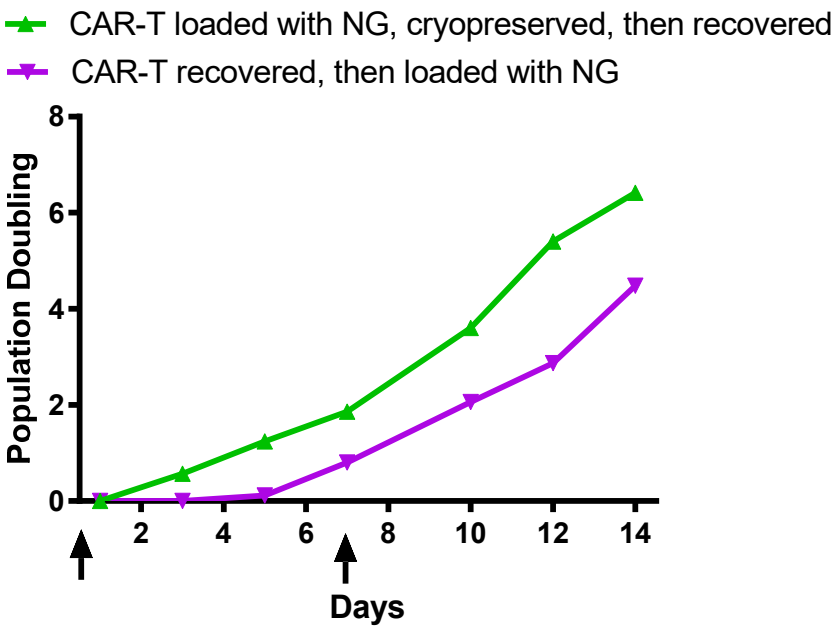

Supplementary Fig. 17. NG-backpacked CAR T-cells can be cryopreserved and recovered, retaining nanogel bioactivity. EGFR-specific human CAR T-cells with or without attached IL-15Sa NGs were frozen and then thawed 7 days later. On thawing, the non-backpacked T-cells were loaded with fresh aCD45/IL-15Sa-NGs (8.5 µg/106 T-cells)and both backpacked T-cell populations were placed in culture with irradiated U87 cells on day 0, with additional feeder cells added on Day 7. CAR T cell expansion was followed by cell counts over time. Shown are one representative of two independent experiments.

Supplementary Table 1. Incorporation efficiency and loading of IL-2Fc in nanogel and liposome formulations.

Formulation	Incorporation effic.[a]	Loading[b]
IL2-Fc-NG	94.0%	~91.5%
IL2-Fc/liposome	0.97%	0.22%

[a]Incorporation efficiency = (incorporated IL-2Fc)/(total IL2-Fc added in preparation). The amount of incorporated IL-2Fc was determined using HPLC by subtracting the non-incorporated IL-2Fc from the total amount. [b]Loading = (mass of incorporated IL2-Fc)/(total mass of NG or liposome).

Supplementary Table 2. Hydrodynamic size and ξ-potential of IL-15Sa-NGs before and after surface modification[a]. Data represent the mean ± SD (n = 3).

surface modification	Size (nm)	zeta potential (mV)
before	89.6 ± 9.3	-10.3
after	121.0 ± 13.1	7.03

[a] The surface modification with anti-CD45 and PEG-PLL is shown in **Figure 2e**.

Supplementary Table 3. Coupling of NGs with or without surface modification of PEG-PLL to T-cells.

Entry	PEG-PLL/IL15-Sa (mol/mol)	[PEG-PLL] (μg/μL)	Coupling efficiency[a]	Density of coupled NG[b] (μg/1.0×10^6 cells)
1	0	0	13.1%	1.31
2	0.08	0.014	76.8%	7.68

[a]Coupling efficiency = (incorporated NG)/(total NG added in preparation). [b]Density of coupled NG = (mass of coupled NG on T-cell surface)/(number of total T-cells).

Supplementary Scheme 1. Synthesis of NHS-SS-NHS crosslinker.